Citation: Molecular Therapy—Nucleic Acids (2013) 2, e99; doi:10.1038/mtna.2013.25

www.nature.com/mtna

METHODS: ORIGINAL ARTICLE

Triple Bioluminescence Imaging for *In Vivo* Monitoring of Cellular Processes

Casey A Maguire[1,2], M Sarah Bovenberg[1–3], Matheus HW Crommentuijn[1,2,4], Johanna M Niers[1,2,4], Mariam Kerami[1,2,4], Jian Teng[1,2], Miguel Sena-Esteves[5], Christian E Badr[1,2] and Bakhos A Tannous[1,2,6]

Bioluminescence imaging (BLI) has shown to be crucial for monitoring *in vivo* biological processes. So far, only dual bioluminescence imaging using firefly (Fluc) and *Renilla* or *Gaussia* (Gluc) luciferase has been achieved due to the lack of availability of other efficiently expressed luciferases using different substrates. Here, we characterized a codon-optimized luciferase from *Vargula hilgendorfii* (Vluc) as a reporter for mammalian gene expression. We showed that Vluc can be multiplexed with Gluc and Fluc for sequential imaging of three distinct cellular phenomena in the same biological system using vargulin, coelenterazine, and D-luciferin substrates, respectively. We applied this triple imaging system to monitor the effect of soluble tumor necrosis factor-related apoptosis-inducing ligand (sTRAIL) delivered using an adeno-associated viral vector (AAV) on brain tumors in mice. Vluc imaging showed efficient sTRAIL gene delivery to the brain, while Fluc imaging revealed a robust antiglioma therapy. Further, nuclear factor-κB (NF-κB) activation in response to sTRAIL binding to glioma cells death receptors was monitored by Gluc imaging. This work is the first demonstration of trimodal *in vivo* bioluminescence imaging and will have a broad applicability in many different fields including immunology, oncology, virology, and neuroscience.

Molecular Therapy—Nucleic Acids (2013) **2**, e99; doi:10.1038/mtna.2013.25; published online 18 June 2013
Subject Category: Methods

Introduction

Bioluminescence imaging (BLI) using luciferase reporters has been indispensible for noninvasive monitoring of different biological processes such as tumor volume and transcriptional activation during tumor development/therapy, as well as immune cell infiltration into the tumor environment.[1] Unlike endpoint analysis, BLI provides real-time, noninvasive assessment of *in situ* biological events, thereby giving a better "picture" of the kinetics of an entire process. Great strides have been made since the first demonstration of *in vivo* BLI.[2] For example, as few as 10 cells expressing firefly luciferase (Fluc) can be detected in deep tissue in some animal models.[3] Additional progress has been made by the discovery and molecular construction of different luciferases with a multitude of properties, including secreted reporters such as *Gaussia* luciferase (Gluc),[4] multicolor light emission spectra for better tissue penetrance *in vivo* and spectral deconvolution,[5,6] increased thermostability,[7] and light output.[8,9] One limitation to current bioluminescence imaging is that typically only one and at most two luciferase reporters are used to measure one or two parameters.[10–12] As tumor formation is a complex process, concurrent measurement of several events will be important for the development of novel therapeutics and their transition to the clinic.

In this study, we have characterized a codon-optimized *Vargula hilgendorfii* luciferase (Vluc) for mammalian gene expression, and showed that this luciferase can be multiplexed with Gluc and Fluc for sequential imaging of three different biological processes in the same biological system. We then applied this triple imaging system to monitor the effect of adeno-associated virus (AAV)-mediated soluble tumor necrosis factor-related apoptosis-inducing ligand (sTRAIL) therapy against intracranial glioma tumors.

Results

Characterization of a codon-optimized Vluc for mammalian gene expression

We first cloned Vluc cDNA, codon-optimized for mammalian gene expression, into a lentivirus vector under the control of the cytomegalovirus promoter (Lenti-Vluc). This vector also expresses the mCherry fluorescent protein separated from Vluc by an internal ribosomal entry site, used to monitor transduction efficiency. Since Vluc cDNA carries a natural signal sequence,[13] it is secreted to the conditioned medium once expressed in mammalian cells. We first observed the level of Vluc secretion by transducing 293T cells with Lenti-Vluc and evaluating the Vluc levels in cell lysates and conditioned medium using the vargulin substrate. We observed that the majority of Vluc activity (78%) was contained in the medium fraction showing efficient secretion (**Figure 1a**). Next, we evaluated the light emission kinetics of Vluc over time and observed a slow decay in light emission, with 44% of the initial signal

[1]Experimental Therapeutics and Molecular Imaging Laboratory, Neuroscience Center, Department of Neurology, Massachusetts General Hospital, Boston, Massachusetts, USA; [2]Program in Neuroscience, Harvard Medical School, Boston, Massachusetts, USA; [3]Department of Neurosurgery, Leiden University Medical Center, Leiden, The Netherlands; [4]Neuro-oncology Research Group, Department of Neurosurgery, VU Medical Center, Cancer Center Amsterdam, Amsterdam, The Netherlands; [5]Department of Neurology, University of Massachusetts Medical School, Worcester, Massachusetts, USA; [6]Center for Molecular Imaging Research, Department of Radiology, Massachusetts General Hospital, Boston, Massachusetts, USA. Correspondence: Bakhos A Tannous, Department of Neurology, Neuroscience Center, Massachusetts General Hospital/Harvard Medical School, Building 149, 13th Street, Boston (Charlestown), Massachusetts 02129, USA. E-mail: btannous@hms.harvard.edu
Keywords: bioluminescence imaging; firefly luciferase; Gaussia luciferase; Vargula luciferase
Received 14 January 2013; accepted 3 May 2013; advance online publication 18 June 2013. doi:10.1038/mtna.2013.25

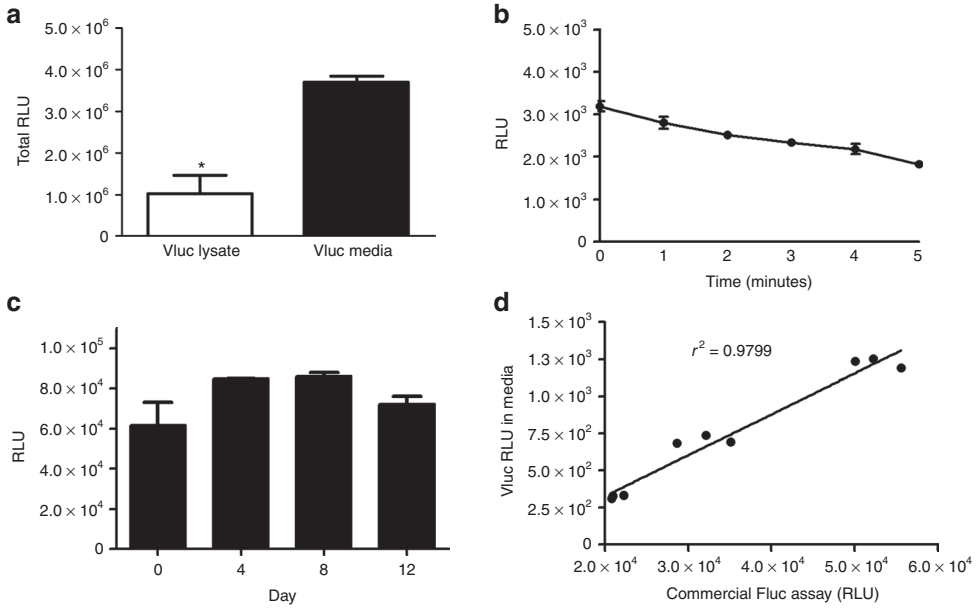

Figure 1 ***In vitro*** **characterization of Vluc-catalyzed luminescence.** (**a**) Vluc assay was performed on conditioned medium as well as cell lysates from 293T cells transduced with a lentivirus vector encoding Vluc to determine the fraction (in RLU) of Vluc being secreted ($n = 3$; $^*P = 0.003$). (**b**) Vluc light emission kinetics was performed by adding the vargulin substrate to Vluc-containing media ($n = 3$). (**c**) Stability of Vluc enzyme was determined by assaying an aliquot of Vluc-containing cell-free conditioned medium, incubated at 37 °C, at different time points ($n = 3$). The slight increase observed between day 0 and 4 is not statistically significant ($P = 0.176$). (**d**) Vluc-based viability assay. 10^5 U87 cells expressing Vluc were seeded in 12-well plates and an aliquot of conditioned medium was assayed for Vluc activity over time. For comparison, a commercially available Fluc-based viability assay was performed on the same cells from which Vluc-media was isolated ($n = 3$ per time point). RLU, relative light unit.

remaining 5 minutes after substrate addition (**Figure 1b**). To further characterize Vluc as a mammalian cell reporter, we measured the stability of the enzyme over time at 37 °C. Conditioned medium from cells expressing Vluc were incubated at 37 °C in a humidified cell incubator. Aliquots were taken at different time points and assayed for Vluc activity. We observed that Vluc levels retained full activity over 12 days indicating high enzyme stability in conditioned medium (**Figure 1c**), similar to that reported for the secreted *Gaussia* luciferase.[14] We next evaluated Vluc as a reporter to monitor cell viability and proliferation over time. U87 glioma cells transduced with Lenti-Vluc were seeded in a culture well and aliquots of conditioned media were collected at different time points and analyzed for Vluc activity. In parallel, a commercially available Fluc-based viability assay was performed for comparison. We observed a high correlation ($r^2 = 0.98$) between the Vluc assay and the established viability assay (**Figure 1d**).

Optimization of the triple *in vivo* bioluminescence imaging system

To validate Vluc as a reporter for *in vivo* imaging, we first characterized its bioluminescence reaction properties in a quantitative tumor model. Nude mice were injected subcutaneously with 2×10^6 U87 cells stably expressing Vluc (through transduction with Lenti-Vluc). Ten days later, mice were injected intravenously (iv; through retro-orbital route) or intraperitoneally (ip) with vargulin (4 mg/kg body weight) and imaged using a cooled charge-coupled device camera at different time points. For iv injected mice, we observed the peak luminescent signal immediately upon injection of vargulin, which rapidly declined to 25% of initial signal by 6 minutes and down to 10% by 26 minutes (**Figure 2a**). For ip injected vargulin, the peak occurred 14 minutes after substrate injection (**Figure 2a**). The peak signal for iv route was 2.5-fold higher than for ip injection. Thus, vargulin was injected iv throughout the study for Vluc imaging.

We then evaluated the possibility of multiplexing Vluc with Gluc and Fluc for triple bioluminescence imaging by measuring the specificity of each luciferase for its substrate *in vivo*. U87 cells stably expressing Vluc, Gluc, or Fluc (under control of the cytomegalovirus promoter) were implanted subcutaneously in nude mice at three different sites. Ten days later, mice were imaged first for Fluc-mediated bioluminescence imaging after ip injection of D-luciferin (200 mg/kg body weight) and acquiring photon counts 10 minutes after injection. Intense luminescence was detected only from tumors expressing Fluc (**Figure 2b**). Twenty-four hours later, mice were imaged immediately after iv injection of coelenterazine (5 mg/kg body weight), and again signal was obtained only from tumor-expressing Gluc (**Figure 2b**). Finally, after another 24 hours, mice were iv injected with vargulin (4 mg/kg body weight) and imaged immediately, which showed a signal only in tumor-expressing Vluc (**Figure 2b**). Quantification of the luciferase signal from each tumor revealed that Fluc and Gluc mediated similar bioluminescence signal, whereas Vluc had a significantly lower signal (~100-fold lower; $n = 3$ mice; $P = 0.016$; **Figure 2c**).

Sequential monitoring of three biological events in response to glioma therapy

We applied the triple luciferase reporter system to monitor glioma response to a gene therapeutic approach using the secreted soluble variant of the anticancer agent TRAIL.[15] We

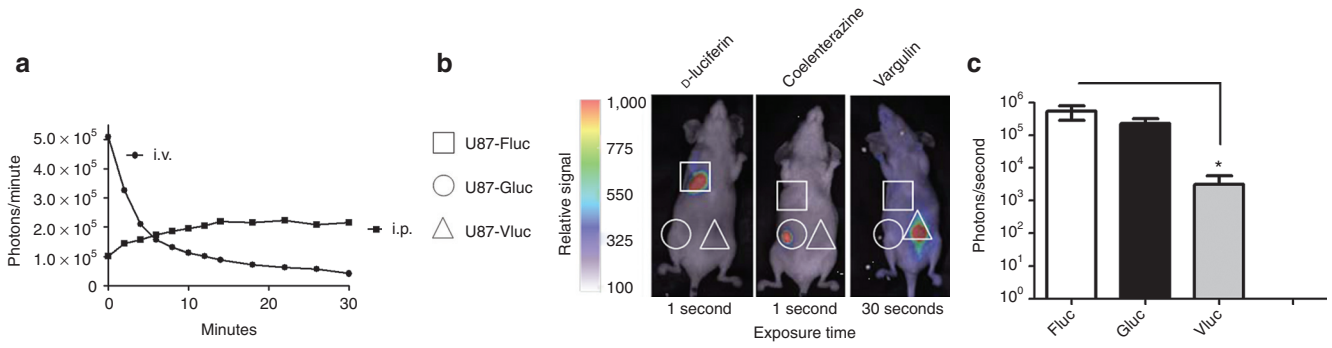

Figure 2 Triple *in vivo* bioluminescence imaging. (**a**) 2×10^6 U87 glioma cells stably expressing Vluc were implanted subcutaneously in nude mice. Tumor-associated Vluc signal after iv or ip injection of 4 mg/kg vargulin is shown by a representative mouse from each injection route ($n = 3$). (**b**) U87 glioma cells stably expressing Gluc, Vluc or Fluc were injected subcutaneously in nude mice at different sites. Ten days later, sequential imaging of Fluc, Gluc, and Vluc was performed (1 day apart) after injection of D-luciferin, coelenterazine, and vargulin. A representative mouse from each imaging session is shown ($n = 3$). (**c**) A region of interest (ROI) was drawn around each tumor location and photons/second were calculated.

first cloned sTRAIL under control of the constitutively active chicken β-actin (CBA) promoter into an AAV2 inverted terminal repeat-flanked transgene cassette and pseudotyped it with an AAVrh.8 capsid (AAV-sTRAIL; **Figure 3a**). As a control, we packaged a similar vector expressing green fluorescent protein (GFP) driven by the CBA promoter. We next cloned Vluc cDNA under control of CBA promoter in another AAV2 vector pseudotyped with AAVrh.8 capsid (AAV-Vluc; **Figure 3a**). Vluc was used as a marker for gene transfer. We then engineered U87 glioma cells to stably express Fluc (U87-Fluc) under control of cytomegalovirus promoter using a lentivirus vector (**Figure 3a**). Fluc was used as a marker for tumor volume. Since TRAIL is known to activate a series of events including the nuclear factor-κB (NF-κB) pathway, we engineered a lentivirus vector expressing Gluc under the control of five tandem repeats of NF-κB responsive elements (**Figure 3a**) as described,[16] and used it to transduce the U87-Fluc cells generating U87-Fluc/NF-Gluc cells. To determine the functionality of the AAV-sTRAIL construct, we transduced U87 cells with 10^4 genome copy (gc)/cell of AAV-sTRAIL or AAV-GFP control vector. Three days later, conditioned media from these cells were harvested and analyzed for TRAIL expression using an ELISA kit. We observed a TRAIL concentration of 124 ng/ml from conditioned medium of AAV-sTRAIL infected cells, while it was undetectable in the media from AAV-GFP control cells, displaying the proper expression and secretion of sTRAIL into the conditioned medium of cells (data not shown). Transfer of conditioned media from U87 cells transduced with AAV-sTRAIL onto fresh U87 cells provided a modest (~25%) yet significant ($P = 0.0035$) killing effect (**Supplementary Figure S1**).

We then stereotactically implanted 10^5 U87-Fluc/NF-Gluc cells into the striatum of nude mice and allowed tumor formation. Nineteen days later, mice were randomly divided into two groups ($n = 5$/group). The first group was infused into the same coordinates used for tumor implantation with 10^{10} gc of both AAV-Vluc + AAV-GFP (AAV-Vluc/GFP; serves as a negative control for therapy). The second group of mice was infused with 10^{10} gc of both AAV-Vluc (to monitor successful gene delivery) and AAV-sTRAIL (antitumor therapy; AAV-Vluc/sTRAIL). As a control, a set of mice was injected only with AAV-GFP vector. Ten days after vector injection, we monitored AAV gene delivery by injecting mice (iv) with vargulin substrate and immediately imaging using a cooled charge-coupled device camera. Evident bioluminescent signal (average radiance of 5×10^5 p/second/cm^2/sr ± 2.3×10^4) was seen at the injection site of all AAV-Vluc injected mice, and not the AAV-GFP controls, showing successful gene delivery (**Figure 3b**). Mice in both groups were monitored for tumor growth (Fluc imaging) at week 2 post-vector injection (corresponding to week 4 post-tumor injection), which showed a robust antitumor response in mice treated with AAV-Vluc/sTRAIL as compared with the control group (AAV-Vluc/GFP; **Figure 3c**).

TRAIL binding to its death receptors recruits TNFR1-associated death domain protein (TRADD) leading to NF-κB activation.[17] We therefore sought to detect NF-κB induction and therefore TRAIL binding to glioma cells in our model. We first confirmed the functionality of the NF-Gluc construct by incubating U87-Fluc/NF-Gluc cells with tumor necrosis factor-α, a known activator of NF-κB, and showed a specific induction of Gluc expression 48 hours after treatment (**Figure 3d**). Next, mice in both the AAV-Vluc/GFP (control) and AAV-Vluc/sTRAIL groups were imaged 22 days and 23 days after AAV injection for Fluc and Gluc, respectively. An increase in Fluc signal was observed at this time point, showing that tumors regained resistance to sTRAIL therapy (data not shown). As expected, specific Fluc bioluminescence at the tumor location was observed in both groups of mice, but visible Gluc signal was detected only in mice injected with AAV-Vluc/sTRAIL and not AAV-Vluc/GFP control animals, indicating binding of sTRAIL to glioma cells and induction of the downstream NF-κB pathway (**Figure 3e,f**). All together, these results show that the triple luciferase system developed here could be used to image three independent cellular processes sequentially in the same animal model.

We next performed an extensive analysis of AAV-mediated sTRAIL therapy in mice bearing intracranial U87 tumors. Ten mice were injected with 5×10^4 U87-Fluc/NF-Gluc cells into the striatum as above, and 14 days later, mice were randomized into two groups ($n = 5$/group) where the first group was infused into the same tumor implanted site with 10^{10} gc of a combination of AAV-Vluc/GFP and the second group with the same amount of AAV-Vluc/sTRAIL. Mice were imaged at day 2, 7, 14, and 21 after vector injection for tumor-associated

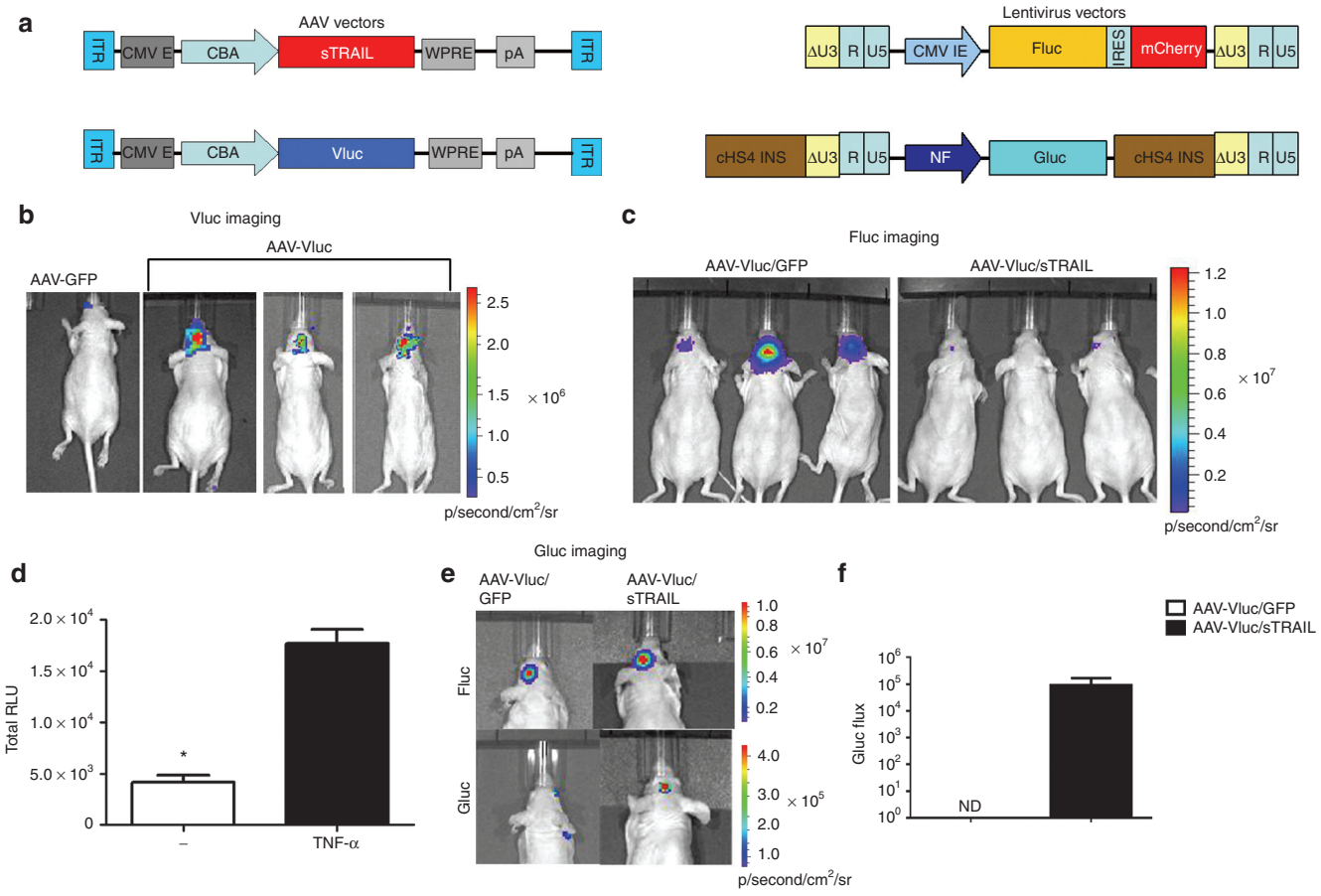

Figure 3 Monitoring of sTRAIL-mediated gene therapy with triple bioluminescence imaging. (**a**) Schematic diagram for the different AAV (left) and lentivirus (right) vector constructs used in this study. AAV vectors: CMV E, cytomegalovirus enhancer; CBA, chicken β-actin promoter; WPRE, woodchuck hepatitis virus posttranscriptional regulatory element; pA, bGH poly A signal. Lentivirus vectors: Diagrams shown represent integrated provirus. CMV IE, cytomegalovirus immediate early promoter; cHS4 INS, chicken β globin hypersensitive site 4 insulator sequence; NF, nuclear factor-κB inducible promoter. (**b–f**) 10^5 U87-Fluc/NF-Gluc glioma cells were implanted intracranially in nude mice. Nineteen days later, the mice brains were infused at the same tumor injection site with 10^{10} gc of either AAV-Vluc/GFP, AAV-Vluc/sTRAIL, or AAV-GFP alone. (**b**) Vluc bioluminescence imaging performed 10 days after vector injection confirming AAV-mediated gene delivery. (**c**) Two weeks post-vector injection, tumor volume was imaged by Fluc bioluminescence imaging. (**d**) Confirmation of NF-Gluc construct. U87-Fluc/NF-Gluc cells in culture were treated with or without tumor necrosis factor-α (TNF-α) (10 ng/ml). Forty-eight hours later, conditioned medium were collected and assayed for Gluc activity to detect levels of NF-κB induction (*$P = 0.0001$). (**e**,**f**) NF-Gluc imaging, a marker for TRAIL binding on glioma cells performed after iv injection of coelenterazine. Calculation of NF-κB activation in glioma-bearing mice treated with AAV-Vluc/sTRAIL or AAV-Vluc/GFP shown in **f**. Note that no Gluc signal was detected in the AAV-Vluc/GFP mice at any time point. Representative mice from each group are showing in (**b**,**c**, and **e**; $n = 5$/group). ITR, inverted terminal repeat; nd, not detected.

Fluc signal. Similar to the first experiment, AAV-mediated sTRAIL expression slowed the tumor growth as compared with control mice. At day 2 after vector injection, the AAV-Vluc/GFP control group had a twofold higher signal ($P = 0.46$) as compared with the AAV-Vluc/sTRAIL-treated mice (**Figure 4a**,**b**). This difference increased to 6.13- ($P = 0.048$) and 33.7-fold ($P = 0.0008$) on day 7 and 14, respectively. All mice in the AAV-Vluc/GFP group were sacrificed between day 14 and 21 after vector injection due to tumor burden, while the entire group in AAV-Vluc/sTRAIL remained alive. Interestingly, the AAV-Vluc/sTRAIL group showed a 193-fold increase in the Fluc signal (and therefore tumor growth) between days 14 and 21, presumably due to U87-gained resistance to sTRAIL therapy (**Figure 4a**,**b**). We also performed an experiment with a higher input of U87 cells and obtained similar results (**Supplementary Figure S2**). We confirmed the luminescence data with a survival analysis, which revealed a significant survival increase ($P = 0.0088$) for mice injected with AAV-Vluc/sTRAIL compared with AAV-Vluc/GFP controls (**Figure 4c**). The median survival time for the AAV-Vluc/GFP group was 35 days while it was 80 days for the AAV-Vluc/sTRAIL group.

Discussion

Luciferases have played a major role in advancing our understanding of biological processes. A broader array of biocompatible, nontoxic, and efficiently expressed reporters that can be used together with existing luciferases can serve to expand this potential. The present study demonstrates for the first time a triple luciferase reporter system for *in vivo* bioluminescence imaging. We showed that *Vargula* luciferase could be multiplexed with *Gaussia* and firefly luciferases for sequential monitoring of three distinct biological phenomena. We also showed

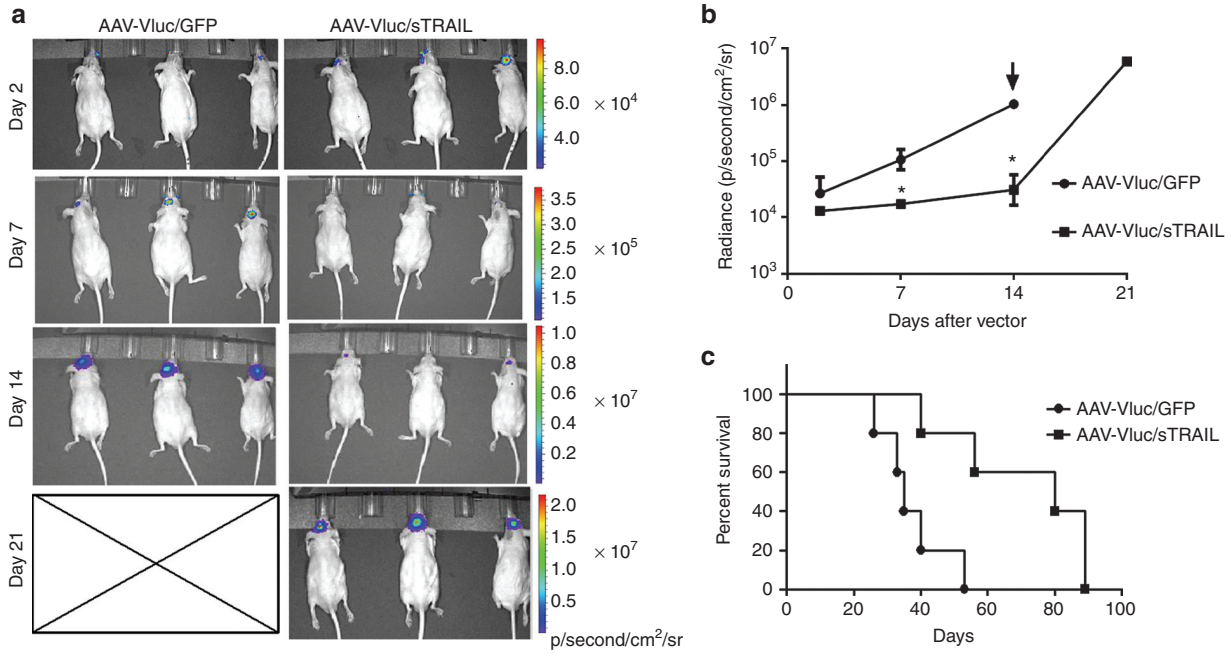

Figure 4 Effect of AAV-sTRAIL vector on U87 glioma tumors. (**a**,**b**) 5×10^4 U87 glioma cells expressing Fluc, a marker for tumor volume, were implanted in the brain of nude mice. Fourteen days later, mice were randomized into two groups and infused into the same tumor injection site with either AAV-Vluc/GFP or AAV-Vluc/sTRAIL ($n = 5$/group). Mice were imaged for Fluc at days 2, 7, 14, and 21 after vector injection. (**a**) Representative set of mice from each group are shown. Note that the scale is different for each time point in order to show the tumor site. (**b**) Quantitation of brain tumor-associated Fluc signal in mice over time. The arrow indicates that all mice in the AAV-Vluc/GFP group were sacrificed between week 2 and week 3 due to tumor burden (*$P = 0.048$ at day14 and *$P = 0.0008$ at day 21). (**c**) Survival analysis of mice bearing U87 glioma tumors treated with either AAV-Vluc/GFP or AAV-Vluc/sTRAIL ($n = 5$; $P = 0.0088$). All Graphs are generated from a representative data set of three independent experiments.

that this triple bioluminescence imaging system yield specific, and detectable bioluminescence signal in deep tissues such as the brain (with intact skull, ~3.5 mm) of mice. Finally, we applied these reporters to monitor three cellular processes in an orthotopic brain tumor model in response to AAV-sTRAIL therapy, thus validating the system for different applications.

Since the cloning and sequencing of *Vargula* (formerly *Cypridina*) *hilgendorfii* cDNA in 1989,[13] several reports have demonstrated the usefulness of this enzyme for luminescence assays.[18–21] However, to our knowledge, no reports have applied it for *in vivo* imaging in mammals, probably owing to the unavailability of its substrate vargulin, which is now commercially available. Vluc cDNA possess a signal sequence and therefore it is naturally secreted from cells allowing real time, multi–time point analysis from the same well.[18,22] In this study, we characterized a codon-optimized Vluc cDNA for mammalian gene expression and showed Vluc to be very stable with no significant decline in activity over 12 days in cell-free conditioned media at 37 °C. Despite that the majority of Vluc was found in the conditioned media of cells due to its native signal sequence, the intracellular Vluc level was efficient for *in vivo* imaging. In applications where higher sensitivity is required, a membrane-bound variant of Vluc[22] could be used, which should yield higher cellular activity similar to recent reports for *Gaussia* luciferase.[23,24]

Several systems for multimodal imaging exist, which incorporate different technologies such as fluorescence, bioluminescence, positron emission tomography, and magnetic resonance imaging.[25] While substantial multiparameter information can be gained by these systems, they have several drawbacks, including higher cost (e.g., magnetic resonance imaging), logistical concerns such as short half-life of some positron emission tomography probes, and broad technical expertise. While fluorescent reporter-based imaging as well as luciferases emitting at different wavelengths can be used for multimodal applications, they require expensive and complicated instrumentation with spectral deconvolution to visualize each biological parameter.[26,27] Furthermore, fluorescence-based imaging is limited by a high background noise due to tissue autofluorescence as well as single animal analysis. On the other hand, BLI has low-to-no background and is thus more sensitive for deep tissue applications.[28] The triple *in vivo* bioluminescence imaging system described here yields multiparameter information distinguished by sequential imaging using different specific substrates, while remaining both cost-effective and highly sensitive, as well as being user friendly; only a simple charge-coupled device camera is required with no need for sophisticated instrument hardware/software. Moreover, this same system can be extended and applied to any field to monitor three distinct biological phenomena in small animals. It is important to note, however, that we have tested Vluc expression in the brain of mice bearing intracranial tumors. Since tumors may have comprised the integrity of the blood–brain barrier, it would be important to evaluate vargulin in a model with intact blood–brain barrier to validate the ability of this substrate in crossing this biological barrier. Another drawback of the triple-reporter system is

the need of methanol to dissolve the vargulin and coelenterazine substrates, limiting imaging frequency due to potential toxicity of the alcohol. The use of water-soluble coelenterazine[29] or the development of similar vargulin substrate would alleviate this issue.

TRAIL has been regarded as an anticancer agent; however, significant cancer types, including gliomas, are resistant to TRAIL-induced cell death.[30] Mechanisms of resistance include downregulation of death receptors,[29] decoy receptor expression,[30] as well as overexpression of the caspase-8 inhibitor, c-FLIP, due to deregulation of the mTOR signaling pathway.[31] In addition, NF-κB induction by TRAIL has been reported as a tumor cell resistance mechanism.[32,33] Another disadvantage of using TRAIL for brain tumor therapy is its inability in crossing the blood–brain barrier. In this study, we circumvented this problem by delivering sTRAIL directly to brain tumor environment using AAV-mediated gene delivery. We chose to use AAVrh.8 as we have previously shown that this serotype yields excellent transduction efficiency of murine normal brain.[34] Injection of AAVrh.8 into the tumor results in transduction of primarily neuronal cells surrounding the tumor.[34] The transduced neurons serve as a therapeutic reservoir surrounding the tumor by synthesizing and secreting sTRAIL, which in turn will find and bind its death receptor present specifically on glioma cells. Despite this continuous release of the anticancer agent by the normal brain, we observed that tumors acquired resistance to sTRAIL therapy; however, a significant increase in survival was observed using AAV-mediated expression of sTRAIL compared with the control group. The exact mechanism of TRAIL resistance in this model is currently not known, but may involve NF-κB signaling, as mice injected with AAV-Vluc/sTRAIL showed activation of the NF-κB transcription factor, as monitored by Gluc imaging. It is noteworthy to mention that U87 cells showed low sensitivity to sTRAIL-mediated death in culture, as compared with the initial high sensitivity *in vivo*. This apparent discrepancy may be explained by several factors. The culture experiment used conditioned medium from cells secreting sTRAIL (124 ng/ml as determined by ELISA) and therefore the cells will only get a "one-shot" delivery, given that toxicity of TRAIL to glioma cells is dose-dependent.[35] Similar results were reported by Yang *et al.* (25% killing) using a dose of 100 ng/ml of sTRAIL in culture.[36] Although the level of AAV-mediated sTRAIL expression in the brain is unknown, the transduction efficiency of the vector serotype used (AAVrh.8) is very high in the murine brain.[37] Similar to our findings, Yang *et al.* reported that despite this apparent low TRAIL-sensitivity *in vitro*, an increase in survival rate *in vivo* was observed when using mesenchymal stem cell to deliver sTRAIL to U87 gliomas.[36] Finally, resistance factors that allow glioma cell survival in culture may not suffice for *in vivo* tumor growth in a complex multicellular environment.

In conclusion, we have developed a triple luciferase system for *in vivo* bioluminescence applications. We showed that each of these luciferases (Vluc, Gluc, and Fluc) is specific to its own substrate and can be multiplexed together to monitor three distinct biological events in the same biological system. This reporter system could be extended to different fields where simultaneous monitoring of multiple parameters is required.

Materials and methods

Cells. U87 human glioblastoma cell line and 293T human kidney fibroblast cells were obtained from the American Type Culture Collection (Manassas, VA). Both cell lines were cultured in high glucose Dulbecco's modified Eagle's medium (Invitrogen, Carlsbad, CA) supplemented with 10% fetal bovine serum (Sigma, St Louis, MO) and 100 U/ml penicillin, 100 µg/ml streptomycin (Invitrogen) in a humidified atmosphere supplemented with 5% CO_2 at 37 °C.

AAV vectors and lentivirus vectors. The AAV-CBA-Vluc vector was constructed by replacing EGFP in AAV-CBA-EGFP[38] with the human codon-optimized Vluc cDNA (a kind gift from Dr Rampyari Walia; Targeting Systems, El Cajon, CA). AAV-CBA-sTRAIL vector consists of a transgene cassette for soluble, secreted TRAIL carrying amino acid (aa) 1–150 from human Flt3L, an isoleucine zipper domain, and the extracellular domain (aa 114–281) of the human TRAIL designed based on previously reported h-Flex-zipper-TRAIL.[15] In all AAV vectors, gene expression is controlled by a hybrid cytomegalovirus enhancer/CBA. All vectors carry a woodchuck hepatitis virus post-trancriptional regulatory element (WPRE) downstream of the transgene. AAV vector stocks were produced by cotransfection of 293T cells by calcium phosphate precipitation of vector plasmid, a mini-adenovirus helper plasmid pFΔ6 (from Dr Weidong Xiao, University of Pennsylvania Medical Center, Philadelphia, PA), and AAVrh.8 helper plasmid pAR8 as described.[38] AAV2/rh.8 vectors were purified and titered as described,[38] yielding typical titers of 10^{13} genome copies (gc) per milliliter.[34] For sTRAIL expression in culture, AAV vectors were packaged as AAV2 since this serotype is known to transduce cells in culture much more efficiently as compared with AAV2/rh.8.

U87Fluc-mCherry cells stably and constitutively expressing both firefly luciferase (Fluc) and mCherry were generated by transduction with lentiviral vector CSCW2-Fluc-ImCherry, which has been previously described.[34] U87Fluc-mCherry cells were subsequently transduced with a lentivirus previously described as Lenti-NF-Gluc, which encodes a Gluc transgene cassette driven by five tandem repeats of NF-κB–responsive elements.[16] This double-transduced U87 cells is referred to as U87Fluc/NF-Gluc cells. The lentivirus vector encoding Vluc was constructed by replacing the Fluc insert in CSCW2-Fluc-ImCherry with the human codon-optimized Vluc cDNA. We achieve >95% transduction efficiency of U87 cells at a multiplicity of infection of 10 with the different lentivirus constructs. We do not find it necessary to sort the cells owing to this high transduction rate.

In vivo tumor models. All animal experiments were approved by the Massachusetts General Hospital Subcommittee on Research Animal Care following guidelines set forth by the National Institutes of Health Guide for the Care and Use of Laboratory Animals. Six to 8 weeks old athymic nude mice were anesthetized with a mixture of ketamine (100 mg/kg) and xylazine (5 mg/kg) in 0.9% sterile saline. For subcutaneous tumors, mice were injected with 100 µl of a 50:50 mixture of Matrigel Basement Membrane Matrix (BD Biosciences, Franklin Lakes, NJ) and 1–2 million U87 cells expressing

Gluc, Vluc, or Fluc resuspended in Opti-MEM. For the brain tumor model, 10^5 U87Fluc/5NF-Gluc cells (in 2 µl Opti-MEM) were intracranially injected in the left midstriatum of nude mice using the following coordinates from bregma in millimeters: anteroposterior +0.5, mediolateral +2.0, and dorsoventral –2.5. These injections were performed using a Micro 4 Microsyringe Pump Controller (World Precision Instruments, Sarasota, FL) attached to a Hamilton syringe with a 33-gauge needle (Hamilton, Reno, NV) at a rate of 0.2 µl/min. Before AAV vector injection, mice were randomized into separate groups by placing all mice into a single cage by one operator and selected for each group by a different operator. For AAV vector injections, mice were anesthetized as above and injected intracranially with 10^{10} gc of each vector using the same coordinates as for tumor injections. AAV vectors were infused at a rate of 0.2 µl/min using a Micro 4 Microsyringe Pump Controller attached to a Hamilton syringe with a 33-G needle.

In vitro and in vivo luciferase imaging. D-luciferin was purchased from Gold Biotechnology (St Louis, MO) and resuspended at 25 mg/ml in phosphate-buffered saline. For Fluc imaging, mice were injected ip with 200 mg/kg body weight of D-luciferin solution, and imaging was performed 10 minutes later. Coelenterazine was obtained from NanoLight™ Technology (Pinetop, AZ) and resuspended at 5 mg/ml in acidified methanol. For Gluc imaging, mice were injected iv (through retro-orbital route) with 5 mg/kg body weight of coelenterazine solution diluted in phosphate-buffered saline and imaging was performed immediately. Vargulin substrate was obtained from NanoLight Technology or from Targeting Systems and was resuspended at 5 mg/ml in acidified methanol. For monitoring cell proliferation with Vluc, we refreshed the media of cells 4 hours before measurements to avoid accumulation of the reporter. For Vluc *in vivo* imaging, mice were injected iv (unless otherwise noted) with 4 mg/kg body weight (diluted in phosphate-buffered saline), and imaging was performed immediately. For sequential imaging of all three reporters, we imaged Fluc on day 1, Gluc on day 2, and Vluc on day 3, allowing 24 hours waiting period between the different imaging sessions. Imaging was performed using an IVIS Spectrum optical imaging system fitted with an XGI-8 Gas Anesthesia System (Caliper Life Sciences, Hopkinton, MA). Bioluminescent images were acquired using the autoexposure function. Data analysis for signal intensities, and image comparisons were performed using Living Image software (Caliper Life Sciences). To calculate radiance for each animal, regions of interest were carefully drawn around each signal, which is expressed as radiance (photons/second/cm^2/steradian).

TRAIL ELISA. The functionality of the AAV-sTRAIL vector was tested by transducing U87 cells with 10^4 gc/cell with AAV2-sTRAIL or a negative control vector AAV2-GFP. Three days later, media was harvested from all wells and a Quantikine Human TRAIL ELISA (R&D Systems, Minneapolis, MN) was performed as per the manufacturer's instructions.

Data presentation and calculations. For experiment in **Figure 1a**, we calculated total relative light unit (RLU) in media and cell lysate as follows: (RLU/volume assayed) × total volume in cell lysate or media. To calculate the percentage of secreted Vluc, we used the following equation: (Total RLU in media)/(Total RLU in media + Total RLU in cell lysate) × 100.

To calculate Gluc Flux in **Figure 3f**, we first divided Fluc values (tumor size) for each mouse to the lowest Fluc value of the three mice (arbitrarily set to one). Next the Gluc values were divided by each of the adjusted values to get the Gluc flux, which was adjusted for tumor size.

Statistical analysis. Statistical analysis was performed using GraphPad Prism version 5.01 software (La Jolla, CA). For comparisons between two samples, an unpaired two-tailed *t*-test was performed. A P value of <0.05 was considered to be statistically significant. For analysis between multiple groups, a one-way analysis of variance was performed followed by a Bonferroni's multiple comparison test to compare two groups.

Supplementary material

Figure S1. U87 glioma cells are moderately sensitive to killing by conditioned media from donor cells transduced with AAV-sTRAIL.
Figure S2. Effect of AAV-sTRAIL vector in mice bearing U87 glioma tumors.

Acknowledgments. This work was supported by grant from National Institutes of Health/National Institute of Neurological Disorders and Stroke (NINDS) P30NS045776 and 1R01NS064983 (B.A.T.) and by a Fellowship from the American Brain Tumor Association (C.A.M.). M.S.B. was supported by a Fulbright scholarship, the Huygens Scholarship Program, VSB fonds, and the Saal van Zwanenberg Foundation. We thank Hiroaki Wakimoto for the GBM8 cells. We acknowledge the Neuroscience Center Nucleic Acid Quantitation Core and Image Analysis Core (supported by NINDS P30NS045776). The authors declared no conflict of interest.

1. Badr, CE, Hewett, JW, Breakefield, XO and Tannous, BA (2007). A highly sensitive assay for monitoring the secretory pathway and ER stress. *PLoS ONE* **2**: e571.
2. Contag, CH, Contag, PR, Mullins, JI, Spilman, SD, Stevenson, DK and Benaron, DA (1995). Photonic detection of bacterial pathogens in living hosts. *Mol Microbiol* **18**: 593–603.
3. Rabinovich, BA, Ye, Y, Etto, T, Chen, JQ, Levitsky, HI, Overwijk, WW *et al.* (2008). Visualizing fewer than 10 mouse T cells with an enhanced firefly luciferase in immunocompetent mouse models of cancer. *Proc Natl Acad Sci USA* **105**: 14342–14346.
4. Tannous, BA, Kim, DE, Fernandez, JL, Weissleder, R and Breakefield, XO (2005). Codon-optimized Gaussia luciferase cDNA for mammalian gene expression in culture and *in vivo*. *Mol Ther* **11**: 435–443.
5. Loening, AM, Wu, AM and Gambhir, SS (2007). Red-shifted Renilla reniformis luciferase variants for imaging in living subjects. *Nat Methods* **4**: 641–643.
6. Branchini, BR, Southworth, TL, Khattak, NF, Michelini, E and Roda, A (2005). Red- and green-emitting firefly luciferase mutants for bioluminescent reporter applications. *Anal Biochem* **345**: 140–148.
7. Branchini, BR, Ablamsky, DM, Murtiashaw, MH, Uzasci, L, Fraga, H and Southworth, TL (2007). Thermostable red and green light-producing firefly luciferase mutants for bioluminescent reporter applications. *Anal Biochem* **361**: 253–262.
8. Kim, SB, Suzuki, H, Sato, M and Tao, H (2011). Superluminescent variants of marine luciferases for bioassays. *Anal Chem* **83**: 8732–8740.
9. Loening, AM, Fenn, TD, Wu, AM and Gambhir, SS (2006). Consensus guided mutagenesis of Renilla luciferase yields enhanced stability and light output. *Protein Eng Des Sel* **19**: 391–400.
10. Vilalta, M, Jorgensen, C, Dégano, IR, Chernajovsky, Y, Gould, D, Noël, D *et al.* (2009). Dual luciferase labelling for non-invasive bioluminescence imaging of mesenchymal stromal

cell chondrogenic differentiation in demineralized bone matrix scaffolds. *Biomaterials* **30**: 4986–4995.
11. Wendt, MK, Molter, J, Flask, CA and Schiemann, WP (2011). *In vivo* dual substrate bioluminescent imaging. *J Vis Exp* **56**: 3245.
12. Bhaumik, S, Lewis, XZ and Gambhir, SS (2004). Optical imaging of Renilla luciferase, synthetic Renilla luciferase, and firefly luciferase reporter gene expression in living mice. *J Biomed Opt* **9**: 578–586.
13. Thompson, EM, Nagata, S and Tsuji, FI (1989). Cloning and expression of cDNA for the luciferase from the marine ostracod Vargula hilgendorfii. *Proc Natl Acad Sci USA* **86**: 6567–6571.
14. Wurdinger, T, Badr, C, Pike, L, de Kleine, R, Weissleder, R, Breakefield, XO *et al.* (2008). A secreted luciferase for ex vivo monitoring of *in vivo* processes. *Nat Methods* **5**: 171–173.
15. Wu, X, He, Y, Falo, LD Jr, Hui, KM and Huang, L (2001). Regression of human mammary adenocarcinoma by systemic administration of a recombinant gene encoding the hFlex-TRAIL fusion protein. *Mol Ther* **3**: 368–374.
16. Badr, CE, Niers, JM, Tjon-Kon-Fat, LA, Noske, DP, Wurdinger, T and Tannous, BA (2009). Real-time monitoring of nuclear factor kappaB activity in cultured cells and in animal models. *Mol Imaging* **8**: 278–290.
17. Chaudhary, PM, Eby, M, Jasmin, A, Bookwalter, A, Murray, J and Hood, L (1997). Death receptor 5, a new member of the TNFR family, and DR4 induce FADD-dependent apoptosis and activate the NF-kappaB pathway. *Immunity* **7**: 821–830.
18. Inouye, S, Ohmiya, Y, Toya, Y and Tsuji, FI (1992). Imaging of luciferase secretion from transformed Chinese hamster ovary cells. *Proc Natl Acad Sci USA* **89**: 9584–9587.
19. Thompson, EM, Nagata, S and Tsuji, FI (1990). Vargula hilgendorfii luciferase: a secreted reporter enzyme for monitoring gene expression in mammalian cells. *Gene* **96**: 257–262.
20. Thompson, EM, Adenot, P, Tsuji, FI and Renard, JP (1995). Real time imaging of transcriptional activity in live mouse preimplantation embryos using a secreted luciferase. *Proc Natl Acad Sci USA* **92**: 1317–1321.
21. Tanahashi, Y, Ohmiya, Y, Honma, S, Katsuno, Y, Ohta, H, Nakamura, H *et al.* (2001). Continuous measurement of targeted promoter activity by a secreted bioluminescence reporter, Vargula hilgendorfii luciferase. *Anal Biochem* **289**: 260–266.
22. Ura, S, Ueda, H, Kazami, J, Kawano, G and Nagamune, T (2001). Single cell reporter assay using cell surface displayed Vargula luciferase. *J Biosci Bioeng* **92**: 575–579.
23. Santos, EB, Yeh, R, Lee, J, Nikhamin, Y, Punzalan, B, Punzalan, B *et al.* (2009). Sensitive *in vivo* imaging of T cells using a membrane-bound Gaussia princeps luciferase. *Nat Med* **15**: 338–344.
24. Niers, JM, Chen, JW, Lewandrowski, G, Kerami, M, Garanger, E, Wojtkiewicz, G *et al.* (2012). Single reporter for targeted multimodal *in vivo* imaging. *J Am Chem Soc* **134**: 5149–5156.
25. Weissleder, R and Pittet, MJ (2008). Imaging in the era of molecular oncology. *Nature* **452**: 580–589.
26. Gammon, ST, Leevy, WM, Gross, S, Gokel, GW and Piwnica-Worms, D (2006). Spectral unmixing of multicolored bioluminescence emitted from heterogeneous biological sources. *Anal Chem* **78**: 1520–1527.
27. Ntziachristos, V (2006). Fluorescence molecular imaging. *Annu Rev Biomed Eng* **8**: 1–33.
28. Badr, CE and Tannous, BA (2011). Bioluminescence imaging: progress and applications. *Trends Biotechnol* **29**: 624–633.
29. Ding, L, Yuan, C, Wei, F, Wang, G, Zhang, J, Bellail, AC *et al.* (2011). Cisplatin restores TRAIL apoptotic pathway in glioblastoma-derived stem cells through up-regulation of DR5 and down-regulation of c-FLIP. *Cancer Invest* **29**: 511–520.
30. Chamuleau, ME, Ossenkoppele, GJ, van Rhenen, A, van Dreunen, L, Jirka, SM, Zevenbergen, A *et al.* (2011). High TRAIL-R3 expression on leukemic blasts is associated with poor outcome and induces apoptosis-resistance which can be overcome by targeting TRAIL-R2. *Leuk Res* **35**: 741–749.
31. Panner, A, James, CD, Berger, MS and Pieper, RO (2005). mTOR controls FLIPS translation and TRAIL sensitivity in glioblastoma multiforme cells. *Mol Cell Biol* **25**: 8809–8823.
32. Zhang, L and Fang, B (2005). Mechanisms of resistance to TRAIL-induced apoptosis in cancer. *Cancer Gene Ther* **12**: 228–237.
33. Ibrahim, SM, Ringel, J, Schmidt, C, Ringel, B, Müller, P, Koczan, D *et al.* (2001). Pancreatic adenocarcinoma cell lines show variable susceptibility to TRAIL-mediated cell death. *Pancreas* **23**: 72–79.
34. Maguire, CA, Meijer, DH, LeRoy, SG, Tierney, LA, Broekman, ML, Costa, FF *et al.* (2008). Preventing growth of brain tumors by creating a zone of resistance. *Mol Ther* **16**: 1695–1702.
35. Badr, CE, Wurdinger, T and Tannous, BA (2011). Functional drug screening assay reveals potential glioma therapeutics. *Assay Drug Dev Technol* **9**: 281–289.
36. Yang B, Wu X, Mao Y, Bao W, Gao L, Zhou P *et al.* (2009). Dual-targeted antitumor effects against brainstem glioma by intravenous delivery of tumor necrosis factor-related, apoptosis-inducing, ligand-engineered human mesenchymal stem cells. *Neurosurgery* **65**: 610–624; discussion 624.
37. Cearley, CN, Vandenberghe, LH, Parente, MK, Carnish, ER, Wilson, JM and Wolfe, JH (2008). Expanded repertoire of AAV vector serotypes mediate unique patterns of transduction in mouse brain. *Mol Ther* **16**: 1710–1718.
38. Broekman, ML, Comer, LA, Hyman, BT and Sena-Esteves, M (2006). Adeno-associated virus vectors serotyped with AAV8 capsid are more efficient than AAV-1 or -2 serotypes for widespread gene delivery to the neonatal mouse brain. *Neuroscience* **138**: 501–510.

Supplementary Information accompanies this paper on the Molecular Therapy–Nucleic Acids website (http://www.nature.com/mtna)